

Green Synthesis of Porous Fe₂O₃/Au Nanocomposite with Chitosan Template using *Gliricidia Sepium* Leaf Aqueous Extract and its Catalytic Activity for the Reduction of 4 Nitrophenols

Purnomo Arif Abdillah¹, Yoki Yulizar²
{purnomo.arif@ui.ac.id¹, yokiy@sci.ui.ac.id²}

Department of Chemistry, Faculty of Mathematics and Natural Sciences (FMIPA),
Universitas Indonesia. Kampus UI Depok, Depok 16424, Indonesia

Abstract. In this work, the green synthesis of porous Fe₂O₃/Au nanocomposite was carried out by reacting Fe(NO₃)₃· with *Gliricidia sepium* leaf aqueous extract and chitosan template using the sol-gel method. After the gel formation, the samples were calcined at 700°C and modified with AuNP. The synthesized porous Fe₂O₃/Au nanocomposites were characterized using UV-Vis Spectrophotometer, Fourier Transformation Infrared Spectroscopy (FTIR), X-Ray diffraction spectroscopy (XRD), and Scanning electron microscope (SEM). Porous Fe₂O₃/Au nanocomposite was tested for catalytic activity for the reduction reaction model of 4-nitrophenol with NaBH₄. The catalytic activities of the porous Fe₂O₃/Au nanocomposite in reactions were monitored by using UV-Vis spectroscopy. The XRD and FTIR confirm the compound formed is α-Fe₂O₃. It was found that the porous Fe₂O₃/Au can convert up to 79% 4-nitrophenol to 4-aminophenols.

Keywords: Porous Fe₂O₃/Au, Green Synthesis, *Gliricidia sepium* leaf Extract, 4 nitrophenol reduction catalyst

1 Introduction

Recent study [1] shows that porous nanocomposite have better properties than non-porous nanoparticles. With the presence of holes in the particles, it will increase the surface area, thereby increasing the ability of the catalyst properties for 4-nitrophenol reduction [2], increasing the electrode capability of the battery [3], increasing battery capacity[4], and increase the nature of the catalyst and the photo thermal effect [5]. The synthesis of porous nanoparticles was carried out using a template in the form of polysaccharides. In previous research, Mg-doped ZrO₂ nanoparticles had been synthesized using aloe vera extract templates. The template is a polysaccharide molecule in the aloe vera extract so that the zircon nitrate salt precursor sticks to the polysaccharide surface and forms a ball. Polysaccharide molecules are removed by calcination [6]. Chitosan is a linear polysaccharide composed of β 1-4 bonds, which are randomly bound to D glucosamine and N acetyl glucosamine, and can cross-link to produce molecules of certain sizes. Chitosan can be used as a template for the synthesis of Fe₂O₃ nanoparticles using the hydrothermal method. The results obtained were that the particles were more homogeneous and the chitosan template was removed by calcination [7]

Green synthesis method is starting to be commonly used in the synthesis of nanocomposite. The use of natural ingredients or biomasses such as plant extracts, algae and fungi has been used for nanosynthesis [8]. *Gliricidia sepium* (Gamal plant) is a shrub from a

legume relative. Often used as a living fence or shade, this shrub or small tree is growing in many areas of Indonesia. Its leaves contain saponins, alkaloids, and flavonoids [9], which are needed for the green synthesis process of nanoparticles. Previous research used *Gliricidia sepium* leaf extract for AgNP synthesis [10] for anti-bacterial applications.

To assess the catalytic properties of the nanocomposite, the reduction of 4-nitrophenol is chosen as the model reaction. 4-nitrophenol is a colourless to yellowish odourless crystal, having the molecular formula $C_6H_5NO_3$ with a molecular weight of 139.11 g/mol. 4-nitrophenol is a pollutant as a result of waste from the pesticide, pharmaceutical, dye and petroleum industries. 4-nitrophenol is a dangerous pollutant because it is stable in water and harmful to health and the environment[11]. Based on the toxicological studies conducted, 4-nitrophenol can cause blood and kidney disorders, liver damage and eye irritation[12]. Catalytic reduction of 4-nitrophenol with $NaBH_4$ as a reducing agent and will produce the final product in the form of a 4-aminophenol that much less toxic.

In this study, porous Fe_2O_3/Au nanocomposite were synthesized with chitosan templates using the sol-gel method in green synthesis using *Gliricidia sepium* leaf extract as a reduction and capping agent. The activity of the synthesized porous Fe_2O_3/Au nanocomposite was tested for the hydrogenation reaction of 4-nitrophenol and compared with the non-porous Fe_2O_3/Au nanocomposite

2 Method

2.1. Materials

Gliricidia sepium leaf. (GSL) was obtained from Secang district, Magelang, Indonesia. Chitosan was obtained from PT ChiMultiguna. Methanol, n-hexane, were obtained from PT. Brataco. $H AuCl_4$ used in this research was synthesized by dissolving 99.9% Au metal from PT. Antam in aqua regia solvent with HNO_3 and HCl ratio of 1:3. HNO_3 , HCl and $Fe(NO_3)_3 \cdot 9H_2O$ were obtained from Merck. All chemicals were analytical grade and used without further purification.

2.2. Preparation of *Gliricidia sepium* Leaf. (GSL) Extract

About 2 kg of GSL dried in room temperature for one week. The dried leaves were blended to soft powders. GSL powder was macerated in methanol with 1:6 ratio w/v for six days, and mixed constantly. The macerated GSL was filtered and the filtrate was extracted using n-hexane in a separation funnel until it formed two fractions. The separated water fraction was phytochemicals analyzed for its polyphenol, tannin, alkaloid, flavanoid, saponnin, terpenoid, and steroid contents. The water fraction was saturated using vacuum rotary evaporator to remove its water solvent and characterized using FTIR spectroscopy (Shimadzu Prestige 21). The saturated GSL extract was then made into a stock solution with 6% concentration (w/v)

2.3. Preparation colloidal chitosan

Colloidal chitosan was prepared by reacting 3 grams of chitosan powder with one liter of 1% acetic acid solution. The solution then stirred and placed in sonicator in 50°C for 3 hours. The results of the reaction were characterized with Particle Size Analyzer to confirm that colloidal chitosan was formed.

2.4. Synthesis of Fe₂O₃/Au nanoparticles

The synthesis of Fe₂O₃/Au nanoparticles (Fe₂O₃/Au-NP) was carried out by mixing the water fraction of GSL extract into the precursor solution of Fe(NO₃)₃ 0.01 M. The mixture was stirred for 2 hours at a temperature of 80-100°C until solution turns dark brown. The colloidal solution formed is heated for 10 hours at 120°C to evaporate the water. The mixture then calcined at 700°C for 5 hours to obtain Fe₂O₃ nanoparticle powder. 40 mg of Fe₂O₃ nanoparticle powder then dispersed in 98ml of distilled water, and 1ml of 1 x 10⁻³M HAuCl₄ solution was added slowly. The solution was added with 1 ml of GSL extract with continued stirring for 2 hours. The mixture dried at 120°C. After drying, the gel formed was rinsed with distilled water and calcined to remove the remaining organic material from GSL Extract

2.5. Synthesis of porous Fe₂O₃/Au

Colloidal chitosan solution was added with the precursor solution of Fe(NO₃)₃ 0.01 M. The solution was stirred for 2 hours at room temperature. The solution was added with 1 mL of GSL extract and heated at a temperature of 80-100°C until solution turns dark brown. Fe(OH)₃-chitosan which is formed is dried at 10 hours at 120°C to evaporate the water. The mixture then calcined at 700°C for 5 hours to obtain porous Fe₂O₃ powder. 40 mg of porous Fe₂O₃ powder then modified with AuNP with the same method above.

2.6. Catalytic activity

4-nitrophenol reduction was used as a model to test the catalytic activity of the synthesized nanocomposites. The catalyst performance test was carried out with mixing 5 mg of catalyst and 10 mL solutions containing 5 x 10⁻⁵ M 4-nitrophenol and 0.1 M NaBH₄. The solutions immediately transferred to cuvette and recorded its absorption using a UV-Vis spectrophotometer (Shimadzu 2600 series) at wavelength 250 – 550 nm as a function of time.

3 Results and Discussion

3.1 Characterization of GSL Extract

Identification of GSL extract was firstly done by phytochemical test. It is conducted to qualitatively analyze the presence of secondary metabolites in aqueous GSL extract. The result showed that aqueous GSL extract contains flavanoids, alkaloids, polyphenols and saponins. Analysis of functional groups of compound contained in the water fraction GSL using a FTIR spectrophotometer is shown in Figure 1. The GSL FTIR spectrum shows a band at 3354cm⁻¹, due to stretching vibrations of the hydroxyl functional group (-OH) originating from alcohol or phenol, peak at 2933cm⁻¹ by stretching vibrations of the functional group CH *sp*³, peak at 1656cm⁻¹ and 1593cm⁻¹ shows stretching vibrations of the C=C and CC aromatic groups, peak at 1403cm⁻¹ by the stretching vibrations of the CH group of alkanes and peak at 1072cm⁻¹ by the stretching vibrations of the CO groups which derived from esters or glycosides. There is peak in 1035cm⁻¹ from C-N amine stretch. The results of GSL extract FTIR characterization are comparable with previous studies [13]

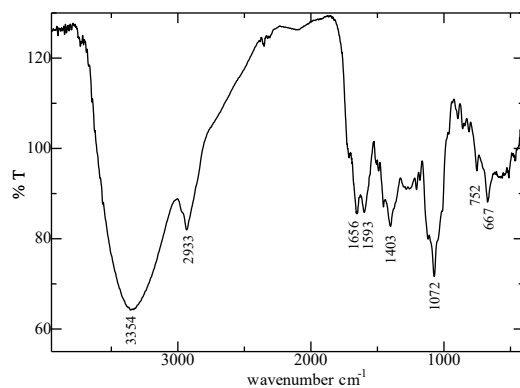


Fig 1. FTIR of GSL Extract

Based on the results, it is known that there are several functional groups in GSL water fraction using FTIR, indicating the presence of secondary metabolites. Identification of saponin compounds is known by the presence of functional groups OH, CH, C = C and CO glycosides [14] while the presence of Alkaloid compounds comes from the presence of CN and C=C groups [15].

3.2 Characterization of Fe₂O₃/Au

FTIR measurements were carried out to determine which functional groups contained in secondary metabolites of GSL extract that play a role in the formation process of Fe₂O₃. The results of the FTIR Fe₂O₃ spectra are shown in Figure 2. In the interaction between GSL extract and Fe-OH, there is a widening and shifting of the peaks of -OH. This shows the interaction of the -OH group from the GSL extract with Fe(OH)₃. This shows that the -OH group acts as a capping agent in the synthesis of Fe₂O₃ NP. Before calcination, Fe(OH)₃ did not have double absorption at around 551 and 467cm⁻¹, which indicates that Fe₂O₃ has not been formed.

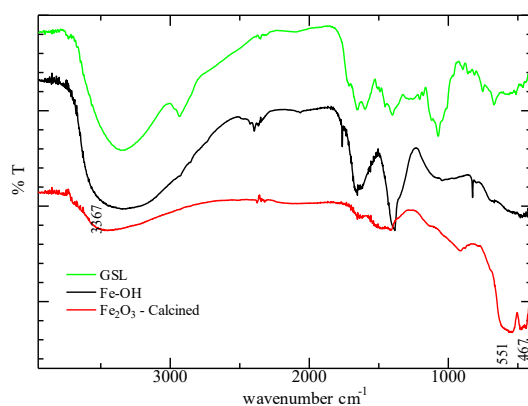


Fig 2. FTIR of GSL extract, Fe(OH)₃ and Calcined Fe₂O₃

The characteristics of Fe-O appeared at 467cm^{-1} and 551cm^{-1} . The spectra at high frequency (551cm^{-1}) is associated with Fe-O deformation at the octahedral and tetrahedral sites, while at lower frequencies (467cm^{-1}) it is derived from Fe-O deformation at the octahedral site of hematite[16]. the different shape of Fe_2O_3 will cause a slight shift in this peak [17]. The wide peak in the Fe_2O_3 spectra around 3300cm^{-1} is the O-H stretching vibration. The peak at 1565cm^{-1} is the absorption of water molecules present in Fe_2O_3 [18]. From the Fe_2O_3 spectra that has been calcined, it can be seen that almost all of the organic material from the GSL has been lost.

The FTIR spectra of porous and nanoparticle Fe_2O_3 modified with AuNP are similar without AuNP (Figure 3 and Figure 4). The absorption at 467 and 551cm^{-1} still derived from Fe-O vibrations. The spectral similarity of the AuNP-modified catalysts is the same as the support, indicating that the addition of AuNP has no or little effect on the hematite bonding. The hole in the porous Fe_2O_3 in other way, make some impurities in the porous $\text{Fe}_2\text{O}_3/\text{Au}$ resulting in the noisier FTIR spectra.

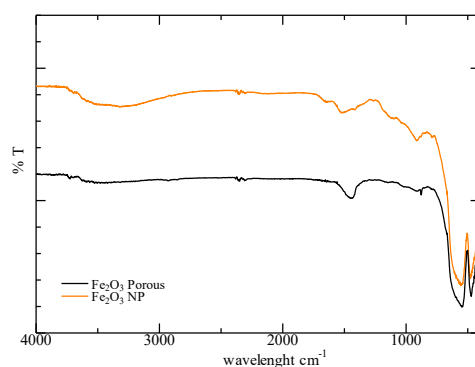


Fig 3. FTIR Porous Fe_2O_3 Porous and Fe_2O_3 NP comparison

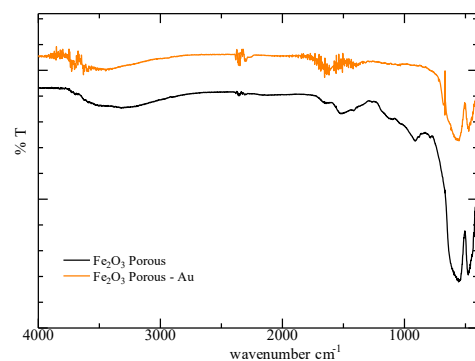


Fig 4. FTIR Porous Fe_2O_3 and Porous $\text{Fe}_2\text{O}_3/\text{Au}$ comparison

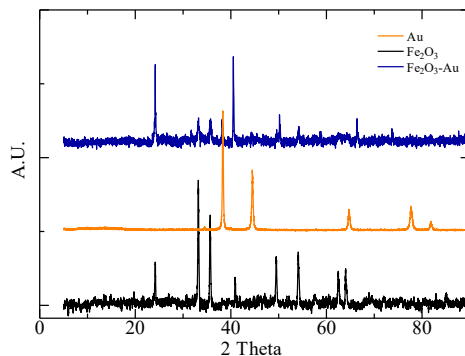


Fig 5. XRD Porous Fe₂O₃, Au and Porous Fe₂O₃/Au comparison

Figure 5 above shows the XRD pattern of the calcined iron oxide powder. All diffraction peaks are in accordance with the α -Fe₂O₃ JCPDS card no. 89-596, indicating that the compound formed is α -Fe₂O₃ [16]. Analysis of the average Fe₂O₃ crystal size is calculated by the Debye-Scherrer equation,

$$D = \frac{K\lambda}{\beta \cos \theta}, \quad (1)$$

Where D is the crystal size, with a K value of 0.9 and a wavelength (Cu) of 1,542 Å, the crystal size of Fe₂O₃ is 62nm. In the porous Fe₂O₃-AuNP composite, the peak intensity of AuNP was weak, because the Au concentration was only 5%. The only significant peak is at an angle of 2θ 38.26° which is the 111 *hkl* plane of the AuNP crystal. There is no new peak in the Fe₂O₃/Au, meaning that no chemical bond exist between Au and Fe₂O₃ molecule. This result conform to FTIR data.

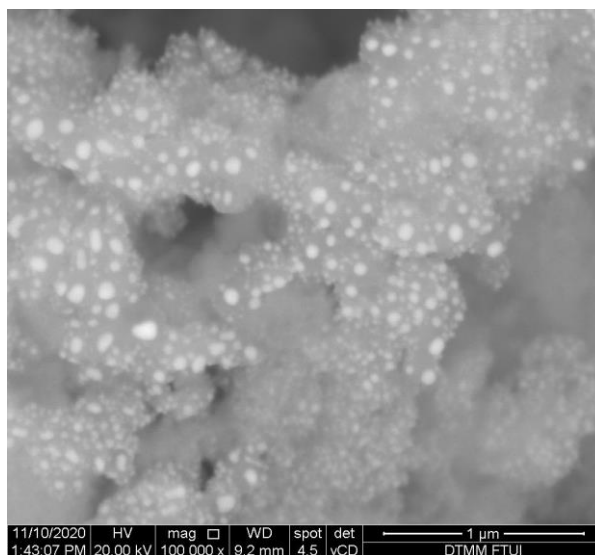


Fig 6 SEM image of porous Fe₂O₃/Au composite

Figure 6 shows the image of porous Fe_2O_3 - AuNP composite. The bright area of the image are the AuNP's. AuNP are scattered evenly on the surface of porous Fe_2O_3 . This immobilized the AuNP in the solution. The size of AuNP obtained ranging between 60 to 200nm.

3.3 Catalytic activity of $\text{Fe}_2\text{O}_3/\text{Au}$

The reduction reaction of 4 nitrophenols using NaBH_4 can be observed using UV-Vis spectroscopy (Figure 7). 4-nitrophenol will change to 4-nitrophenolate ion in alkaline conditions and has a strong absorption at 400nm, the product of this reaction is 4 aminophenol which has a weaker absorption at 300nm. By observing the absorbance of 4 nitrophenolates ion at 400nm, the 4-nitrophenol concentration can be obtained in real time. The percent of 4-nitrophenolate ion that consumed in reaction then plotted with time in Figure 8.

From the results of the reduction reaction NaBH_4 shows that the effectiveness as a reduction catalyst increases with the presence of holes in the material. Having holes increases the surface area which is important for increasing contact with the substrat. Within 60 minutes, it showed that 4 nitrophenols were converted by Fe_2O_3 NP, porous Fe_2O_3 , $\text{Fe}_2\text{O}_3/\text{Au}$ NP, porous $\text{Fe}_2\text{O}_3/\text{Au}$ at 5.5, 7.5, 70 and 79% respectively (Table 1) This figure is still below the AuNP as a reference, because AuNP is a homogeneous catalyst that is evenly distributed in the solution. In addition, the immobilization of AuNP into Fe_2O_3 causes the catalyst to be heterogeneous and reusable.

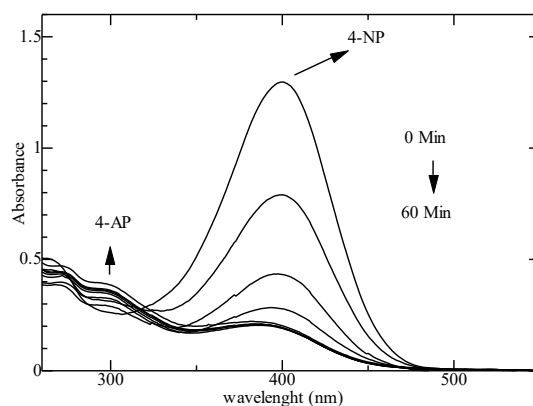


Fig 7. UV spectra of reduction 4NP in 60 minutes

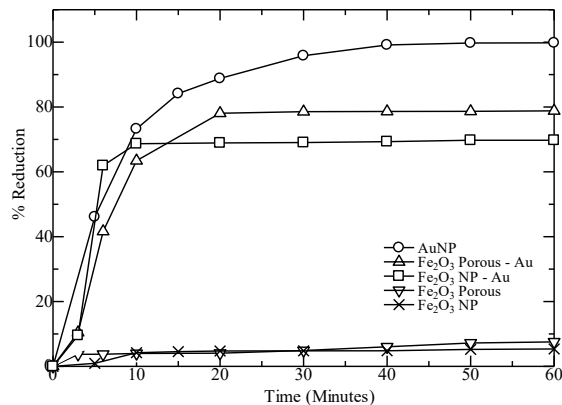


Fig 8. Percent reduction of 4NP with different catalyst

Table 1 Conversion rate of 4NP with different catalyst

catalyst	Reaction time (m)	Conversion (%)
Porous Fe ₂ O ₃ /Au	60	79
Fe ₂ O ₃ /Au NP	60	70
Porous Fe ₂ O ₃	60	7.5
Fe ₂ O ₃ NP	60	5.5
AuNP	60	99

4 Conclusion

Porous Fe₂O₃/Au was successfully synthesized using *Gliricidia sepium* leaf extract and chitosan template using simple and green methods. *Gliricidia sepium* leaf extract contain saponins and flavonoids that act as capping agents to prevent agglomeration of nanoparticles. FTIR and XRD analysis confirmed the formation of α -Fe₂O₃, and the addition of the AuNP doesn't intervene with Fe₂O₃ structure. SEM analysis confirms the presence of AuNP in the surface of Fe₂O₃. From the results of the reduction reaction analysis, the presence of the holes in the porous Fe₂O₃/Au increases its effectiveness as a catalyst in 4-nitrophenol reduction with conversion rate of up to 79%.

Acknowledgements. This work is supported by Saintek scholarship given to the first author from Ministry of Research, Technology, and Higher Education, Indonesia

Reference

- [1] V. Valtchev and L. Tosheva, "Porous Nanosized Particles: Preparation, Properties, and Applications," *Chem. Rev.*, vol. 113, 2013.
- [2] W. Li *et al.*, "Hollow mesoporous SiO₂ sphere nanoarchitectures with encapsulated silver

- nanoparticles for catalytic reduction of 4-nitrophenol," *Inorg. Chem. Front.*, vol. 3, no. 5, pp. 663–670, 2016.
- [3] X. Lin *et al.*, "Templating synthesis of Fe₂O₃ hollow spheres modified with Ag nanoparticles as superior anode for lithium ion batteries," *Sci. Rep.*, no. March, pp. 1–9, 2017.
- [4] B. Koo *et al.*, "Hollow Iron Oxide Nanoparticles for Application in Lithium Ion Batteries," 2012.
- [5] G. K. Larsen, W. Farr, and S. E. Hunyadi Murph, "Multifunctional Fe₂O₃-Au Nanoparticles with Different Shapes: Enhanced Catalysis, Photothermal Effects, and Magnetic Recyclability," *J. Phys. Chem. C*, vol. 120, no. 28, pp. 15162–15172, 2016.
- [6] L. Renuka *et al.*, "Hollow microspheres Mg-doped ZrO₂ nanoparticles: Green assisted synthesis and applications in photocatalysis and photoluminescence," *J. Alloys Compd.*, vol. 672, pp. 609–622, 2016.
- [7] S. Kalarickal Janardhanan, I. Ramasamy, and B. U. Nair, "Synthesis of iron oxide nanoparticles using chitosan and starch templates," *Transit. Met. Chem.*, vol. 33, no. 1, pp. 127–131, 2008.
- [8] S. Irvani, "Green synthesis of metal nanoparticles using plants," *Green Chem.*, vol. 13, no. 10, pp. 2638–2650, 2011.
- [9] P. Aye and M. Adegun, "Chemical Composition and some functional properties of Moringa, Leucaena and Gliricidia leaf meals," *Agric. Biol. J. North Am.*, vol. 4, no. 1, pp. 71–77, 2013.
- [10] R. W. Rajesh, L. R. Jaya, K. S. Niranjana, D. M. Vijay, and B. K. Sahebrao, "Phytosynthesis of Silver Nanoparticle Using Gliricidia sepium (Jacq.)," *Curr. Nanosci.*, vol. 5, no. 1, pp. 117–122, 2009.
- [11] N. Jadbabaei, R. J. Slobodjan, D. Shuai, and H. Zhang, "Catalytic reduction of 4-nitrophenol by palladium-resin composites," *Appl. Catal. A Gen.*, vol. 543, no. May, pp. 209–217, 2017.
- [12] M. Koizumi, Y. Yamamoto, Y. Ito, and M. Takano, "COMPARATIVE STUDY OF TOXICITY OF 4-NITROPHENOL AND 2, 4-DINITROPHENOL IN NEWBORN AND YOUNG RATS," vol. 26, no. 5, pp. 299–311, 2001.
- [13] M. Oladunmoye, K. Ayantola, A. Agboola, B. Olowe, and O. Adefemi, "Antibacterial and Ftir Spectral Analysis of Methanolic Extract of Gliricidia sepium Leaves," *J. Adv. Microbiol.*, vol. 9, no. 4, pp. 1–10, 2018.
- [14] M. S. Almutairi and M. Ali, "Direct detection of saponins in crude extracts of soapnuts by FTIR," *Nat. Prod. Res.*, vol. 29, no. 13, pp. 1271–1275, 2015.
- [15] M. A. G. Maobe, R. M. Nyarango, and P. O. Box, "Fourier Transformer Infra-Red Spectrophotometer Analysis of Urtica dioica Medicinal Herb Used for the Treatment of Diabetes , Malaria and Pneumonia in Kisii Region , Southwest Kenya," vol. 21, no. 8, pp. 1128–1135, 2013.
- [16] A. Mirzaei *et al.*, "Synthesis and characterization of mesoporous α -Fe₂O₃ nanoparticles and investigation of electrical properties of fabricated thick films," *Process. Appl. Ceram.*, vol. 10, no. 4, pp. 209–218, 2016.
- [17] X. Liu, S. Fu, H. Xiao, and C. Huang, "Preparation and characterization of shuttle-like α -Fe₂O₃ nanoparticles by supermolecular template," vol. 178, pp. 2798–2803, 2005.
- [18] K. Raja *et al.*, "Sol-gel synthesis and characterization of α -Fe₂O₃ nanoparticles," *Superlattices Microstruct.*, vol. 86, pp. 306–312, 2015.